Dalton Transactions

PAPER

View Article Online
View Journal

Cite this: DOI: 10.1039/c7dt01459g

Spectroscopic and reactivity differences in metal complexes derived from sulfur containing Triphos homologs†

A. Petuker,‡[a] P. Gerschel,‡[a] S. Piontek,‡[a] N. Ritterskamp,[a] F. Wittkamp,[a] L. Iffland,[a] R. Miller,[a] M. van Gastel[b] and U.-P. Apfel *[a]

Herein, we report a simplified method for the synthesis of Triphos homologs $H_3CC(CH_2X)_n(CH_2Y)_{3-n}$ (X = SPh, Y = PPh_2, n = 0–3). The multidentate compounds were tested for their potential to coordinate metals such as Ni, Fe, and Mo under the same experimental conditions. Cyclic voltammetry, spectroelectrochemical IR investigations as well as DFT calculations were used to examine the electronic alterations in a series of $[\{H_3CC(CH_2X)_n(CH_2Y)_{3-n}\}Mo(CO)_3]$ complexes and to evaluate their potential to open coordination sites or to release CO upon oxidation or in the presence of different solvents. In addition, we demonstrate that the catalytic hydrosilylation of *N*,*N*-dimethylbenzamide to *N*,*N*-dimethylbenzylamine is influenced by the applied tripodal ligand. Our investigations show the high potential of such manipulations to selectively alter the dynamics of the binding properties of Triphos-metal complexes and their reactivity.

Received 23rd April 2017,
Accepted 10th July 2017

DOI: 10.1039/c7dt01459g

rsc.li/dalton

Introduction

Tripodal compounds such as $CH_3C(CH_2PPh_2)_3$ (Triphos, 1,1,1-tris(diphenylphosphinomethyl)ethane) and $CH_3Si(CH_2PPh_2)_3$ ($Triphos^{Si}$, tris(diphenylphosphinomethyl)methylsilane) and their respective metal complexes are receiving increasing attention due to their impressive catalytic properties.[1,2] The ruthenium,[3–12] rhodium,[13–17] molybdenum[18,19] and cobalt[20,21] complexes of these ligands have been particularly well studied and were recently shown to be powerful *e.g.* in the hydrogenation of CO_2 and lactams as well as in the activation of N_2.[10,22] Notably, the potential to switch between κ^2- or κ^3-binding modes was highlighted as one possible explanation for their remarkable performance.[16] Along this line, a flexible, solvent- and temperature-triggered binding of Triphos as well as $Triphos^{Si}$ to metals was observed in their Co- and Fe-complexes.[23,24] As such, these tripodal ligands reveal properties of metalloenzymes allowing for a controlled opening and closing of reactive sites with minimal energetic demands. Therefore, the modulation of the metal–ligand binding strength seems to be a key feature in the tuning of the catalytic properties. A comparable effect on catalysis was recently shown for $[(Triphos)FeCl_2]$ and $[(Triphos^{Si})FeCl_2]$.[24] The modulation of the binding properties due to C/Si exchange in the backbone of the tripodal ligand revealed a significant effect on the metal complexes to support either Sonogashira cross coupling or hydrosilylation reactions. Triphos was shown to have a higher tendency to adopt a κ^3-binding mode as compared to its $Triphos^{Si}$ counterpart.[24] This finding demonstrated the importance of investigating the Triphos-ligand flexibility within catalysis. However, although Triphos is a common ligand framework in catalytic applications, attempts to alter the catalyst's properties, by partially exchanging the phosphine donor groups with other substituents, remain limited. Prominent examples for such a change in reactivity are [(Triphos)Mo(dppm)]-type complexes (dppm = bis(diphenylphosphino)methane) with different substituents on phosphorus that were reported to allow for an activation of N_2.[18,22,25] By modulation of the substitution patterns at the phosphorus donor atoms, a significant alteration of the N–N stretch vibrations was observed, suggesting a substituent-dependent N_2 activation.

Given the impressive catalytic properties of Triphos derived compounds, it is important to develop synthetic pathways for tripodal compounds comprising altered donor sets that are

[a]*Anorganische Chemie I, Ruhr-Universität Bochum, Universitätsstraße 150, D-44801 Bochum, Germany. E-mail: ulf.apfel@rub.de*
[b]*Max-Planck-Institut für Chemische Energiekonversion, Stiftstraße 34-36, 45470 Mülheim, Germany*

†Electronic supplementary information (ESI) available: IR and SEC-IR spectra, GC-MS analysis and X-ray crystallographic analysis. CCDC 1545160–1545164 and 1545379. For ESI and crystallographic data in CIF or other electronic format see DOI: 10.1039/c7dt01459g

‡These authors contributed equally.

both efficient and affordable. Synthetic pathways towards Triphos ligands with mixed substitution patterns, including the ligands presented in this work, have been reported in literature.[22,26–35] The synthetic pathways are, however, long and cumbersome and therefore limit investigation of such ligands in catalytic applications. Furthermore, reactivity changes *via* substitution of the donor atoms remain elusive.[26,29,35–38] In this work, we have focused on a straightforward synthetic route for substitution of phosphorus by sulfur in the ligand series [**SSS**] (1,1,1-tris(phenylthiomethyl) ethane), [**PPP**] (1,1,1-tris(diphenylphosphinomethyl)ethane), [**PSS**] (1-(diphenylphosphinomethyl)-1,1-bis(phenylthiomethyl) ethane) and [**PPS**] (1,1-bis(diphenylphosphinomethyl)-1-bis (phenylthiomethyl)ethane) (Scheme 1). The different donor sets are of interest in redox catalysis due to their different stabilizing properties towards metals.[39–41]

The syntheses of **SSS** and **PPP** were previously reported from 1,3-dichloro-2-(chloro-methyl)-2-methylpropane (**1**) *via* nucleophilic substitution with thiols[42,43] or phosphines.[44] Synthetic access towards the mixed-donor compounds **PSS** and **PPS** is not as straightforward.

Whilst the synthesis of **PSS** was previously reported *via* 3-methyl-3-((phenylthio)methyl)oxetane,[26] synthesis of **PPS** was reported to proceed *via* (2,2,5-trimethyl-1,3-dioxan-5-yl) methyl-4-methylbenzene-sulfonate.[33] The synthetic prerequisites and functionalizations required to perform the lengthy procedures render a simple alteration of metal complexes with tripodal ligands difficult. A possible alternative pathway was reported by Tuczek and coworkers.[22] Starting from the trichloride **1**, a one- or two-fold substitution with $HP^iPr_2{\cdot}BH_3$ allowed for the synthesis of the respective mono- and diphosphines. However, the synthetic route was limited by the steric demand of the borane-protected diisopropyl phosphine and the neopentyl backbone. Likewise, a controlled substitution reaction was reported when compound **1** reacted with stoichiometric amounts of $HPPh_2/KO^tBu$ in DMSO.[36]

To develop tripodal compounds comprising mixed sulfur/phosphorus donor sets, we also started our synthetic approach from the trichloride **1**, a cheap and readily available starting material. We aimed at finding a simple and straightforward synthetic procedure towards all tripodal compounds **SSS**, **PPP**, **PSS** and **PPS** for a stepwise, systematic replacement of the thioether by phosphine groups and investigation of their binding affinities towards metals under varying oxidative conditions. In addition we herein show the different reactive behavior of their iron carbonyl derivatives for the hydrosilylation of *N*,*N*-dimethylbenzamide to *N*,*N*-dimethylbenzylamine.

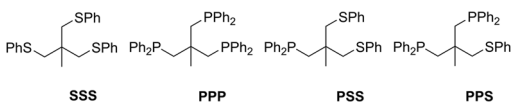

Scheme 1 Tripodal compounds providing [**SSS**], [**PPP**], [**PSS**] and [**PPS**] donor sets.

Results and discussion

Synthesis of the ligands

Compounds **SSS** and **PPP** were synthesized according to literature procedures by reaction of **1** with either excess amounts of thiophenol or lithium diphenylphosphide (Scheme 2).[42–44] Subsequently, we attempted the synthesis of compounds **PSS** and **PPS** applying the routes described by Kabachnik[45] as well as Tuczek[22] and coworkers. While the reaction of **1** with one or two equivalents $HPPh_2/KO^tBu$ in DMSO resulted in the selective formation of compounds **2** and **3**, respectively, subsequent attempts to convert the remaining chlorides into thiophenol containing products **PSS** and **PPS** failed in our hands and solely afforded starting material. This observation can be assigned to the cumulated steric shielding of the neopentyl backbone and the diphenylphosphine moieties. Equally to the synthesis of **2** and **3**, the reaction of compound **1** and stoichiometric amounts of thiophenol, NaH and KI in DMF at 50 °C yielded the one- or twofold substituted compounds **4** or **5** as the main products in 42 and 55% yield, respectively. The reaction conditions are key towards the successful synthesis of both compounds. Variations from the synthetic protocol, *e.g.* by varying the amount of KI used or changing the reaction temperature, lead to different product distributions and commonly resulted in the formation of tri-substituted phosphines, thioethers or no conversion at all. The subsequent treatment of compounds **4** and **5** with potassium diphenylphosphide afforded the desired compounds **PSS** and **PPS** in very good yields (>44% overall yield). In contrast to the literature reported lengthy and cumbersome procedures,[26,33] the herein described pathway thus allows for a simple and straightforward synthesis of **PSS** and **PPS** in only a two-step synthesis.

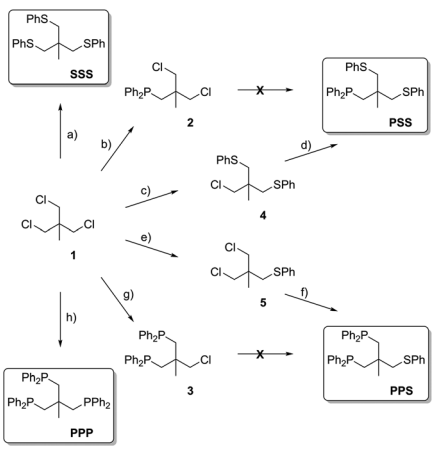

Scheme 2 Reaction scheme towards the syntheses of tripodal compounds with mixed [PS]-donor sets. (a) 3 equiv. NaSPh, 3 equiv. KI, DMF, 60 °C; (b) 1 equiv. $KPPh_2$, DMSO, 60 °C; (c) 2 equiv. NaSPh, 2 equiv. KI, DMF, 100 °C; (d) 1 equiv. $KPPh_2$, DMSO, 100 °C; (e) 1 equiv. NaSPh, 1 equiv. KI, DMF, 100 °C; (f) 2 equiv. $KPPh_2$, DMSO, 100 °C; (g) 2 equiv. $KPPh_2$, DMSO, 100 °C; (h) 3 equiv. $LiPPh_2$, THF, −78 °C.

Reactions with metals and characterization

With the simple synthetic protocol, we were able to efficiently synthesize the ligands **SSS**, **PPP**, **PSS** and **PPS** in gram scale for further coordination studies. We were especially interested in their comparative coordination behavior towards Fe^{II}- and Ni^{II}-salts (Scheme 3). The coordination reactions of Triphos **PPP** with $FeCl_2$ and $[Ni(CH_3CN)_6](BF_4)_2$ are literature reported and selectively afford complexes **6** and **7** in high yields, with the **PPP** ligand in a κ^2-coordinated manner (Scheme 3).[24,46] Likewise, the reaction of ligand **PPS** and $[Ni(CH_3CN)_6](BF_4)_2$ afforded complex **8** that reveals a κ^2-coordinated tripodal ligand.[46] However, in contrast to the previously reported pyramidal complex **7**, compound **8** adopts a square-planar coordination (Fig. 1). In both cases the remaining coordination sites are occupied by CH_3CN molecules – two in the case of the square planar complex **8** and three in the case of the pyramidal complex **7**. As the uncoordinated S/P donor site in **PPP** and **PPS** is electronically isolated from the metal center, in both **7** and **8**, it is unlikely that this change in geometry is due to a change in ligand field strength. This is consistent with the weakly bound nature of the axial CH_3CN molecule in **7**. For **8**, two CH_3CN molecules as well as κ^2-coordinated **PPS** coordinate the Ni^{II} center, revealing Ni–N distances of 1.901(2)/1.905(2) Å and Ni–P distances of 2.1972(5)/2.1921(4) Å. The P(1)–Ni–P(2) (91.84(2)°) and N(1)–Ni–N(2) (90.51(6)°) bond angles give rise to an ideal square planar assembly. In addition, $^{31}P\{^1H\}$ NMR spectroscopy revealed a distinct signal for the coordinated phosphine groups at −15.7 ppm as compared to the phosphorus signals for the free ligand (−27.10 ppm). In contrast, no $^{31}P\{^1H\}$ NMR signal was observed for compound **7**. The electronic differences due to the different ligand field environments are also visible within the UV/vis spectra of **7** and **8**. While **7** possesses two distinct bands at 422 and 728 nm, compound **8** reveals a solitary band at 428 nm (Fig. S1†). A similar coordination behavior of **PPP** and **PPS** is observed upon reaction with $FeCl_2$ yielding the isostructural complexes **6** and **9**. It is also worth to note that the reactions of **PPS** with NiX_2 (X = Cl, Br, I) and $CoCl_2$ have been previously reported.[29] These Ni and Co halide complexes adopted a similar κ^2-coordination involving only the phosphorus donors. Structural analysis of complex **9** unequivocally confirms a tetrahedrally coordinated Fe^{II} center bearing the tripodal ligand **PPS** in κ^2-coordination mode and two additional chloride ions (Fig. 1). The Fe–Cl distances of 2.213(2)/2.241(3) Å and Fe–P distances of 2.432(3)/2.451(3) Å are within the expected range and comparable to those of **6** (Table 1).[46] The ligand **PPS** coordinates iron with both P-atoms as donors, leaving the thioether group uncoordinated. Mössbauer data (δ = 0.59 ± 0.02 mm s^{-1}, ΔE_q = 2.23 ± 0.02 mm s^{-1}) are in line with a high-spin Fe^{II} center.[24,47] Unlike the reactions of compounds **PPP** and **PPS**, the reaction of ligands **SSS** and **PSS** with Fe^{II}- or

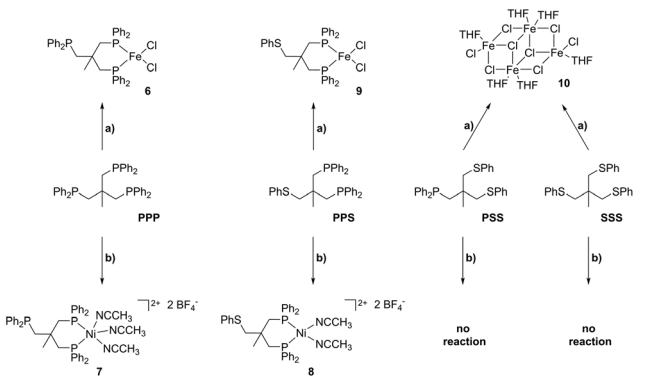

Scheme 3 Ligand controlled synthesis of iron and nickel complexes **6–10** starting from ligands **SSS**, **PPP**, **PSS** and **PPS**. Reaction conditions: (a) $FeCl_2$, THF, 25 °C; (b) $[Ni(CH_3CN)_6](BF_4)_2$, CH_3CN, 25 °C.

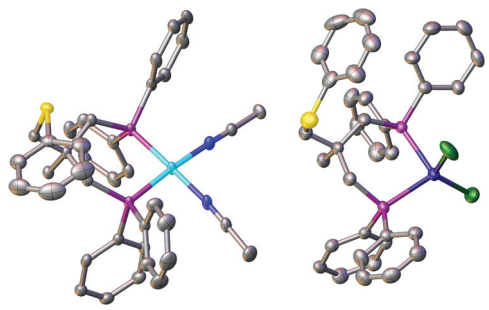

Fig. 1 Molecular structures of compounds **8** (left) and **6** (right) with thermal ellipsoids drawn at the 50% probability level (hydrogen atoms are omitted for clarity). Color code: C gray, S yellow, P purple, Ni turquoise, N blue, Fe dark blue and Cl green.

Table 1 Selected bonding angles and lengths of Fe- and Ni-complexes **6–9**

	Ni		Fe	
	7	**8**	**6**	**9**
Bond lengths [Å]				
M–P(1)	2.1717(7)	2.1921(6)	2.404(2)	2.430(3)
M–P(2)	2.1951(7)	2.1972(6)	2.414(2)	2.452(2)
M–N(1)	1.925(2)	1.905(2)	—	—
M–N(2)	1.928(3)	1.901(2)	—	—
M–N(3)	2.268(3)	—	—	—
M–Cl(1)	—	—	2.218(2)	2.241(3)
M–Cl(2)	—	—	2.253(2)	2.213(3)
Bond angles [°]				
P(1)–M–P(2)	93.12(3)	91.84(2)	91.08(2)	93.57(3)
P(1)–M–N(1)	86.85(7)	87.64(6)	—	—
P(1)–M–N(2)	161.68(9)	172.72(8)	—	—
P(1)–M–N(3)	102.97(7)	—	—	—
P(2)–M–N(1)	171.84(8)	178.29(8)	—	—
P(2)–M–N(2)	89.59(7)	89.80(6)	—	—
P(2)–M–N(3)	98.48(6)	—	—	—
N(1)–M–N(2)	87.93(9)	90.51(8)	—	—
N(1)–M–N(3)	89.47(9)	—	—	—
N(2)–M–N(3)	94.53(11)	—	—	—
P(1)–M–Cl(1)	—	—	113.12(3)	114.2(1)
P(1)–M–Cl(2)	—	—	104.18(3)	98.57(9)
P(2)–M–Cl(1)	—	—	123.69(3)	120.55(8)
P(2)–M–Cl(2)	—	—	94.07(2)	103.37(10)
Cl(1)–M–Cl(2)	—	—	124.39(3)	121.24(11)

Ni^{II}-salts did not result in the formation of the desired complexes. Moreover, the attempted complexation of $FeCl_2$ with both Triphos analogs resulted in the formation of $[Fe_4Cl_8(THF)_6]$ **10** and is in line with reports on the substitutional lability of diphosphine ligands in tetrahedral Fe^{II}-chloro complexes.[48] The results clearly show that the binding affinity of the ligands can be tuned by the simple alterations shown herein. The limited coordination chemistry of **SSS** and **PSS** towards Ni^{II}- and Fe^{II}-salts led us to direct our attention towards another metal that would enable coordination of **SSS**, **PPP**, **PSS** and **PPS**. Mo^0-complexes were previously shown to allow for stable coordination of tripodal ligands comprising a [**SSS**], [**PSS**], [**PPS**] or [**PPP**] donor set and thus allow for comprehensive structural and spectroscopic comparison.[26,28,33,49,50] While a κ^2/κ^3-isomerization of the ligands binding modes of the ligands is feasible by changing the reaction conditions (*e.g.* temperature, solvent, oxidation state, counter ion) and would be in line with our observations on [PPP]Fe- and [PPP]Ni-complexes,[24,46] release of CO was reported for [PPP]$M(CO)_3$ (M = W, Mo) upon oxidation to Mo(III) and formation of seven-coordinate Mo-complexes with Cl_2 or Br_2.[51] This CO-releasing reaction, which is analogous to the chemistry of CO-releasing molecules (CORMs),[52] thus displays a second possibility of $Mo(CO)_3$-moieties comprising the **SSS**, **PPP**, **PSS** or **PPS** ligands to react on altered reaction conditions.

Reaction of compounds **SSS**, **PPP**, **PSS** and **PPS** with 1 equiv. $Mo(CO)_3$(toluene) in THF at room temperature afforded the respective Mo^0-complexes $[Mo(SSS)(CO)_3]$ **11**, $[Mo(PSS)(CO)_3]$ **12**, $[Mo(PPS)(CO)_3]$ **13** and $[Mo(PPP)(CO)_3]$ **14** in good yields (Scheme 4). Structural analysis confirmed a κ^3-coordination mode for all ligands. Notably, binding of **PPS** was solely reported in a κ^2-fashion in an analogue compound to **13**, which was obtained by treatment of the respective ligand and $Mo(CO)_6$.[26] This difference clearly shows that even small changes in the reaction protocol can lead to significant alterations in the product formation. Furthermore, it highlights the importance of comparative evaluations under exactly the same experimental conditions. Analysis of the molecular structures reveals an octahedrally coordinated Mo^0 center bearing the κ^3-bound tripodal ligands **SSS**, **PPP**, **PSS** or **PPS** and three additional CO ligands for all complexes **11**–**14** (Fig. 2 and Table 2). Compound **11** shows Mo–S distances of 2.564(1)/2.571(2)/2.561(1) Å and Mo–C distances of 1.973(9)/1.944(6)/1.968(5) Å with an average C–O distance of 1.153 Å. Similarly, the Mo-complexes **12** and **13** with mixed donor sets reveal Mo–S and Mo–C distances in the same range as observed for **11** (Table 2). While single crystal X-ray diffraction confirmed the composition and coordination mode of compound **14**, the quality of the obtained crystals did not allow for any discussion of bond lengths and angles.

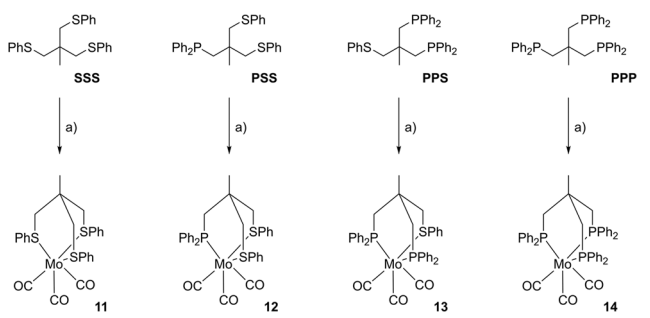

Scheme 4 Synthesis of Mo-complexes with κ^3-bound ligands. Reaction conditions: (a) $[Mo(CO)_3$(toluene)], THF, 25 °C.

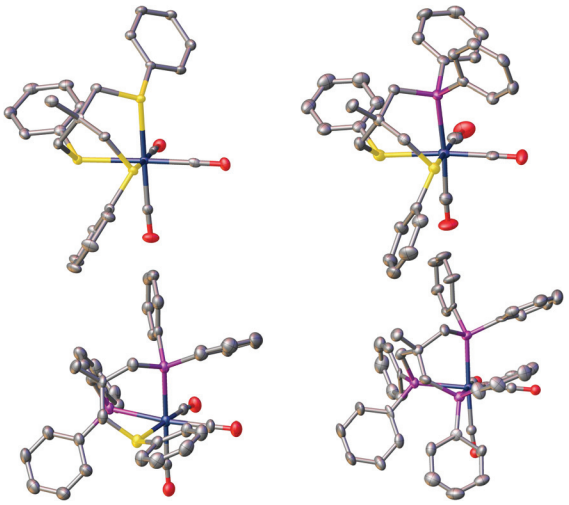

Fig. 2 Molecular structures of compounds **11** (top left), **12** (top right) and **13** (bottom left) as well as the structural motif of **14** (bottom right, CO ligands shown in ball and stick representation) with thermal ellipsoids drawn at the 50% probability level (hydrogen atoms are omitted for clarity). Color code: C gray, S yellow, P purple, Mo blue and O red.

Table 2 Selected bonding angles and lengths of Mo-complexes **11**–**13**

	11	**12**	**13**
Bond lengths [Å]			
Mo–P(1)	—	2.532(1)	2.517(2)
Mo–P(2)	—	—	2.539(2)
Mo–P(3)	—	—	—
Mo–S(1)	2.564(1)	2.5414(9)	2.552(2)
Mo–S(2)	2.571(2)	2.585(1)	—
Mo–S(3)	2.561(1)	—	—
Mo–C(1)	1.973(9)	1.949(4)	1.958(6)
Mo–C(2)	1.944(6)	1.967(4)	1.994(6)
Mo–C(3)	1.968(5)	1.936(4)	1.992(5)
C(1)–O(1)	1.143(8)	1.165(4)	1.124(7)
C(2)–O(2)	1.169(7)	1.159(4)	1.143(8)
C(3)–O(3)	1.148(7)	1.164(4)	1.155(8)
Bond angles [°]			
P(1)–Mo–P(2)	—	—	83.87(5)
P(1)–Mo–P(3)	—	—	—
P(2)–Mo–P(3)	—	—	—
S(1)–Mo–S(2)	76.96(5)	84.64(3)	—
S(1)–Mo–S(3)	87.56(4)	—	—
S(2)–Mo–S(3)	84.94(5)	—	—
P(1)–Mo–S(1)	—	80.30(3)	87.28(5)
P(1)–Mo–S(2)	—	87.02(3)	—
P(2)–Mo–S(1)	—	—	79.99(5)
C(1)–Mo–C(2)	85.8(3)	85.4(2)	85.7(2)
C(1)–Mo–C(3)	84.6(3)	83.5(2)	84.7(2)
C(2)–Mo–C(3)	85.5(2)	87.7(2)	88.7(2)

Table 3 Spectroscopic and electrochemical comparison of complexes **11–14**, and symmetry classification of the CO stretching frequencies according to idealized C_{3v} symmetry

	Infrared spectroscopy ν [cm^{-1}]					$^{31}P\{^1H\}$ NMR δ [ppm]	Mo^0/Mo^I $E_{1/2}$ [V]
	Solid[a]	THF	THF ox.	CH_3CN	CH_3CN ox.	$CDCl_3$	CH_3CN
11	—	—	—	—	2037	—	−0.130
	1925(a_1)	1919	1919	1919	—		
	—	1898	1903	—	—		
	1821(e)	1828	—	—	—		
	1791(e)	1780	1785	1796	—		
12	—	—	1969	—	—	18.5	−0.072
	—	1939	1938	—	—		
	1926(a_1)	1919	1894	1931	1931[b]		
	1837(e)	1837	1835	1830	1830[b]		
	1788(e)	1780	—	1801	1801[b]		
13	—	—	2019	—	1990	18.1	0.068
	1925(a_1)	1939	1938	1930	1933		
	—	1852	1853	1850	—		
	1829(e)	1834	1833	1836	—		
	—	—	—	1817	—		
	—	—	—	1807	—		
14	—	—	2021	—	n.d.	18.1	0.134
	1925(a_1)	1938	1938	1929			
	1831(e)	1844	1850	1838			
	—	—	—	—			

[a] The symmetry of the vibration frequencies was assigned according to an idealized C_{3v} symmetry. [b] The intensity of this band decreased, compared to the spectrum for non-oxidized complexes.

Notably, the stronger π-acceptor nature of the phosphine respective to the thioether donor influences the *trans* located CO ligands. Due to a weaker π-backbonding in this position, Mo–C distances are increased by 0.03 Å compared to the other CO ligands. In addition, $^{31}P\{^1H\}$ NMR spectroscopy showed one signal for the coordinated phosphine groups at ~18 ppm for all complexes **12–14**, indicating electronic equivalence for all Mo-bound phosphorus atoms (Table 3). However, compared to the free ligand (−27.10 ppm) the phosphorus atoms are strongly deshielded. In addition, IR spectroscopy revealed distinct CO bands for complexes **11–14**, which allows evaluation of the donor/acceptor strength of compounds **SSS**, **PPP**, **PSS** and **PPS**. In the solid state, a sharp CO band at 1925 cm^{-1} is uniformly observed for all complexes, and two additional CO bands at lower wavenumbers (~1830 cm^{-1} and ~1790 cm^{-1}) depend on the donor sets of ligands **SSS**, **PPP**, **PSS** and **PPS** (Table 3). For complexes **11** and **12**, which exhibit more sulfur than phosphorus atoms, the band at lower wavenumbers is most intense.

However, if the number of phosphorus atoms increases in complexes **13** and **14**, the CO band at higher wavenumbers becomes dominant with the second band becoming a shoulder. This behavior indicates a weaker π-backbonding character of the CO ligands *trans* to the P-donors and hence supporting the previously mentioned π-acceptor character of the phosphines (Fig. 3A). The observation of weaker π-backbonding to the CO ligands *trans* to the stronger π-acceptor phosphine ligands is consistent with observations for the related compounds (L)W(CO)$_3$ and (L)Mo(CO)$_3$ (L = RX–CH$_2$CH$_2$–Y–CH$_2$CH$_2$XR; Y, X = N, S, P; R = Me, Et).[32] For both complexes, the basicity of the metal center decreased in the order of SR < PR < NR and the thioether groups were reported to be much weaker donors than their corresponding phosphines.

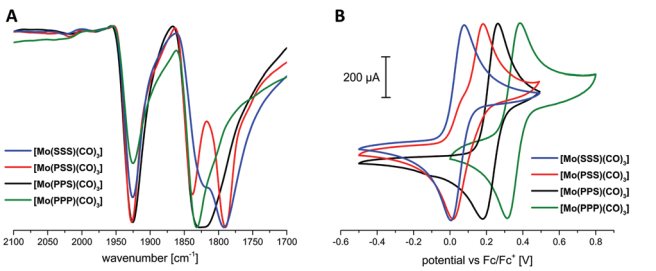

Fig. 3 A: IR spectra of compounds **11–14** in the carbonyl region. B: Cyclic voltammograms of **11–14** in CH_3CN, with 0.1 M $[^nBu_4N]^+PF_6^-$.

Electrochemical investigations on the Mo compounds furthermore support this finding. Cyclic voltammograms of complexes **11–14** in CH_3CN reveal a fully reversible Mo^0/Mo^I redox couple,[39] with gradually increasing redox couples from −0.130 V (**11**), −0.072 V (**12**), 0.068 V (**13**), to 0.134 V (**14**) *vs.* the ferrocene/ferrocenium couple (Fig. 3B and Table 3).

In contrast to thioethers, which act as pure σ-donors,[53,54] the phosphines herein exhibit additional π-acceptor properties[55] resulting in more anodic potentials due to the decreased electron density at the metal center.

κ^2/κ^3-Isomerization *vs.* CO release

The κ^3-coordination mode and altered electrochemical properties directed our interest towards a possible κ^2/κ^3-isomerization *vs.* CO release in different solvents and upon oxidation of

the $Mo(CO)_3$-moieties. Consequently, the Mo-complexes **11–14** were studied in polar (CH_3CN) and unpolar solvents (THF) and changes in coordination were examined by IR spectroscopy (Table 3). Such data provide valuable information on the symmetry and electronic configuration of complexes with tripodal ligands, as was reported *e.g.* for the hemilabile ligand binding at di-iron sites comprising thiol and thioether donors.[56] For that, the CO bands are a valuable probe to judge the binding of the ligands or even loss of CO: while complexes with a κ^3-binding ligand should reveal a maximum of three CO stretching frequencies, complexes with a κ^2-bound ligand should produce a more complex IR spectrum. In contrast, less CO bands or decreased signal intensity should be observable when CO is released. In general, the IR spectra in solution comprised sharper bandwidths than those in the solid state. Whilst complex **11** with a [SSS] donor set reveals CO stretching frequencies at 1919, 1898, 1828 and 1780 cm^{-1} in THF, only two bands at 1919 and 1796 cm^{-1} are observed in CH_3CN (Fig. S2 and S3†). In order to rationalize the number of bands, a DFT calculation was performed for **11**. Likewise, calculations have been performed for **11** as κ^2-isomer with and without coordinated solvent, and for **11** with dissociated CO. The calculations in CH_3CN indicate that the κ^2-isomers with and without coordinating CH_3CN are favored and within 1.5 kcal mol^{-1} of each other (Table S1†). Herein, the calculated IR bands are observed at 1895, 1774 and 1772 cm^{-1} and 1906, 1786 and 1776 cm^{-1}, respectively, and are in good agreement with the experimental findings. Unfortunately, calculations with a specific THF interaction turned out to be not feasible. The more complex band structure found in THF suggests that besides a κ^3-isomer a second complex species is present in solution. Likewise, the band structure of **12** in THF differs clearly from the one in CH_3CN (Fig. 4 and S4†). While compound **12** reveals bands at 1931, 1830 and 1801 cm^{-1} in CH_3CN, comparable to the solid crystalline samples, bands at 1939, 1919, 1837 and 1780 cm^{-1} were observed in THF, suggesting at least a partial formation of another unidentified isomer of **12**. Calculations for **12** reveal that the κ^3-isomer in CH_3CN is most stable with IR bands at 1894, 1798 and 1773 cm^{-1}. The IR bands for complex **13** in THF (1939, 1852, 1834 cm^{-1}) and CH_3CN (1930, 1850, 1836 cm^{-1}) show comparable frequencies assuming a similar conformation in both solvents. Moreover, the IR spectrum of **13** in CH_3CN shows additional frequencies at 1817 and 1807 cm^{-1} also suggesting the presence of an intact κ^3-isomer. This finding is supported in terms of energy by the calculations suggesting the κ^3-isomer to be the most stable one, followed by formation of a κ^2-isomer rather than CO cleavage (Fig. S5, S6 and Table S1†).

Compound **14** reveals significantly shifted bands at 1938 and 1844 cm^{-1} in THF that are comparable with those of **13** in THF (Fig. S7†). In contrast, the spectrum in CH_3CN suggests that the ligand remains bound in a κ^3-configuration with comparable IR bands as observed in the solid IR (1929 and 1838 cm^{-1}). Such findings are further supported by DFT calculations showing the intact κ^3-isomers being energetically favored (Table S1†). While the observed spectroscopic changes are small, it is evident that the solvent has a noticeable influence on the solution structure of the complexes, which is in agreement with previous reports on $Mo^0(CO)_3$ trithioether complexes.[57] Furthermore, the observation of the additional CO bands in different solvents are in accordance with DFT calculations and suggests a κ^2/κ^3-isomerization of the complexes **11**, **12**, **13** and **14** depending on the polar or non-polar solvent system rather than CO release.

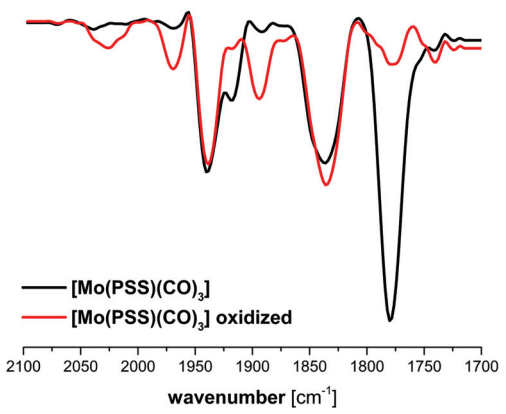

Fig. 4 IR spectrum of compound **12** in THF (black) and spectroelectrochemical IR of **12** upon oxidation at −0.1 V *vs.* Fc/Fc^+ (red).

Spectroelectrochemistry

In order to further investigate effects that trigger the κ^2/κ^3-isomerization and CO release of tripodal ligands, we focused on the alteration of the metal oxidation state as a possible pathway to change the coordination mode of the tripodal ligand. We therefore performed spectroelectrochemical IR measurements on complexes **11–14**. Oxidation of the complexes **11–14** in both THF as well as in CH_3CN result in significant changes in the CO band structure. While complex **11** shows a sharp CO band at 1919 cm^{-1} in CH_3CN, the intensity of this band fades in the oxidized state and an additional band at 2037 cm^{-1} appears (Fig. S3†). This alteration is indicative of a degradation (CO release) that is concomitant with the oxidation of **11**. While calculations indicate that formation of the κ^2-isomer is preferred, it is not unreasonable to assume that a formed κ^2-intermediate as suggested by DFT calculations can subsequently undergo CO release (Table S2†). In THF, only a slight decrease of the CO band intensities at 1828 and 1785 cm^{-1} can be observed over time (Fig. S2†) likewise suggesting degradation *via* an altered intermediate. While this behavior suggests that upon oxidation CO is readily released and is in line with previous observations on CORMs,[58] it is obvious that the solvent has a significant influence on the CO release and the intermediates formed.

In contrast, oxidation of compound **12**, dissolved in THF, affords two new CO bands at 1969 and 1894 cm^{-1} (Fig. 4). Calculations indicate that in this case, the κ^3-isomer is almost isoenergetic with the κ^2-isomer with either the S or P arm being uncoordinated, as well as with the κ^3-complex with

uncoordinated CO (Table S2†). In contrast, oxidation of **12** in CH_3CN does not lead to an altered CO band structure. The decrease in intensity also suggests a degradation of **12** upon oxidation in CH_3CN, but significantly slower compared to **11** (Fig. S4†). When complex **13** is oxidized in THF, the intensity of the bands at 1939, 1852 and 1833 cm^{-1} decreases drastically and a new band at 2019 cm^{-1} is formed (Fig. S5†). Likewise, similar behavior is observed for the oxidation of complex **13** in CH_3CN (Fig. S6†). Again calculations suggest that the energy differences between κ^3, κ^2 and CO uncoordinated species are small and likewise indicate the formation of a complex mixture with all three species being present (Table S2†). During the oxidation of complex **14** in THF, the intensities of the CO bands at 1938 and 1844 cm^{-1} decrease and an additional band at 2021 cm^{-1} is observed (Fig. S7†). Unfortunately, compound **14** in its oxidized form could not be investigated in CH_3CN due to its very low solubility; calculations indicate that the κ^3-complex is most stable, that is in line with the stabilizing effect of the P atoms (Table S2†). The altered number of CO stretching vibrations for the **11–14** suggests a change of the ligands' coordination mode and all complexes **11**, **12**, **13** and **14** show a ligand isomerization or CO release/decomposition upon oxidation in polar solvents resulting in different CO bands. However, the rate as well as the pathway of decomposition/CO release is depending on the number of P atoms in the ligand.

Although showing a similar trend for isomerization/CO release, it is obvious from the altered CO shifts and electrochemical redox potentials for **11–14** that the binding strength of the different ligands **SSS**, **PPP**, **PSS** and **PPS** towards the central metal must be different. Such observations thus show that the complexes' ability to perform ligand isomerization (most likely by adopting either κ^2/κ^3-bound ligands) as well as CO release is controlled by the Triphos-based ligand systems. Such properties can be easily modified by altering the donor sets of the tripodal ligands and render the complexes prone to κ^2/κ^3-isomerization or CO release/decomposition.

Catalysis

As a result of the different metal-binding strength and the observed binding isomerization of ligands **SSS**, **PPP**, **PSS** and **PPS** in Fe^{II}-,[24] Co^{II}-[23] as well as the herein reported Mo^0-complexes, we expected significant alterations also in catalytic applications. As a proof-of-principle study, we also attempted to show the influence of the different donor sets on catalytic applications. While the Mo-complexes **11–14** were never reported for any catalytic application and we did not manage to find any catalytic application for such complexes, Ru-, Rh- and Fe-complexes based on the ligand **PPP** and its Si-derivative are frequently reported catalysts in literature.[1,2] A prominent example herein is the reduction of *N*,*N*-dimethylbenzamide to *N*,*N*-dimethylbenzylamine by iron carbonyls.[59,60] Since the alteration of the substitution pattern clearly showed a difference on the solution stability as well as ligand isomerization and CO release, we thus investigated the reduction of *N*,*N*-dimethylbenzamide to *N*,*N*-dimethylbenzylamine with Ph_2SiH_2 facilitated by $Fe_3(CO)_{12}$. Unfortunately we were not able to isolate the corresponding Fe-complexes and thus performed the reactions in mixtures of 2 mol% $Fe_3(CO)_{12}$ and the ligands **SSS**, **PPP**, **PSS** or **PPS**. However, the alteration of the ligand set is expected to result in a different catalytic performance.

Table 4 Catalytic conversion of *N*,*N*-dimethylbenzamide to *N*,*N*-dimethylbenzylamine with 2 mol% $Fe_3(CO)_{12}$, Ph_2SiH_2 and in the presence/absence of compounds **SSS**, **PSS**, **PPS** or **PPP**. Reactions were performed in toluene under reflux conditions and yields were determined by GC-MS using an external authentic standard. Values were determined in triplicates

Complex	Ligand	Yield of *N*,*N*-dimethylbenzylamine [%]		
		After 1 h	After 3 h	After 16 h
$Fe_3(CO)_{12}$	—	14.1 ± 2.1	24.4 ± 0.5	100
$Fe_3(CO)_{12}$	**SSS**	26.3 ± 2.2	35.8 ± 0.4	100
$Fe_3(CO)_{12}$	**PSS**	4.7 ± 1.2	14.5 ± 1.3	30.7 ± 1.8
$Fe_3(CO)_{12}$	**PPS**	4.8 ± 0.9	12.2 ± 0.8	28.0 ± 1.4
$Fe_3(CO)_{12}$	**PPP**	10.9 ± 0.9	17.0 ± 0.1	90.2 ± 0.8

The respective conversion and yields were determined by GC-MS after 1, 3 and 16 hours (Fig. S8–S11†). While in the absence of any supporting ligand, 14.1 and 24.4% *N*,*N*-dimethylbenzylamine were obtained after 1 and 3 hours, respectively, full conversion was obtained after 16 hours (Table 4). Notably, in the presence of **SSS**, the yield of *N*,*N*-dimethylbenzylamine is significantly increased after 1 hour reaction time as compared to experiments in the absence of any ligand. After 1 hour already a yield of 26.3% of *N*,*N*-dimethylbenzylamine is obtained. After 3 hours the yield is further increased to 35.8% and after 16 hours it reaches 100%. While we are not able to give mechanistic details, this example clearly shows that in the presence of compound **SSS**, the catalytic conversion is significantly faster than in the absence of any ligand, which is also notable by the increased turnover frequency (TOF) (1.1×10^{-3} s^{-1} for $Fe_3(CO)_{12}$ alone and 1.7×10^{-3} s^{-1} for $Fe_3(CO)_{12}$ + **SSS** determined after 3 hours reaction time (Table 5)). While applying the ligand **SSS** has a beneficial effect on the catalytic hydrosilylation, application of the more phosphorus containing ligands **PPP**, **PSS** and **PPS** considerably slow down the reaction. In the presence of compounds **PSS** and **PPS** under the same experimental conditions as used for compound **SSS**, even after 16 hours the desired reduction

Table 5 Turnover numbers (TON) and frequencies (TOF) for the conversion of *N*,*N*-dimethylbenzamide to *N*,*N*-dimethylbenzylamine with 2 mol% $Fe_3(CO)_{12}$, Ph_2SiH_2 and in the presence/absence of compounds **SSS**, **PSS**, **PPS** or **PPP** after 3 hours reaction time

Complex	Ligand	TON	TOF [s^{-1}]
$Fe_3(CO)_{12}$	—	12.2	1.11×10^{-3}
$Fe_3(CO)_{12}$	**SSS**	17.9	1.66×10^{-3}
$Fe_3(CO)_{12}$	**PSS**	7.2	0.67×10^{-3}
$Fe_3(CO)_{12}$	**PPS**	6.1	0.57×10^{-3}
$Fe_3(CO)_{12}$	**PPP**	8.5	0.79×10^{-3}

product was solely obtained in 30.7 and 28.0% yield, respectively (Table 4).

Notably, the higher the phosphorus content, the lower was the maximum yield for *N*,*N*-dimethylbenzylamine obtained after 16 hours. One might assume that the potentially more rigid binding of the ligand to the metal center as well as an increased steric demand (**PPP** > **PPS** > **PSS** > **SSS**) will suppress the coordination of the substrate. However, although not as effective as in the presence of **SSS**, reactions performed in the presence of compound **PPP** reveal an enhanced catalytic reaction and afford a comparable catalytic performance as $Fe_3(CO)_{12}$ itself (Table 4). It is thus currently unclear if the different binding affinity of the ligands will either change the metal complexes involved within catalysis or the substrate binding towards the complexes. Turnover numbers (TON) and frequencies (TOF) decrease according to **SSS** > **PPP** > **PSS** > **PPS** (Table 5). Whilst we are not able to examine the reaction mechanism for the hydrosilylation, we demonstrate, for the first time, that the different coordination of the tripodal **SSS**, **PPP**, **PSS** and **PPS** ligands influences the catalytic hydrosilylation of *N*,*N*-dimethylbenzylamine.

Conclusion

While the tripodal ligand Triphos is commonly used in catalysis,[1] derivatives with altered donor sets were sparsely reported.[26,29,35–38] We herein describe a simple and straightforward two-step synthesis of Triphos homologs comprising mixed [PSS], [PPS] donor sets. Furthermore, we herein show, based on their respective Ni^{II}-, Fe^{II}- and Mo^0-complexes that they comprise differences in their metal binding capability and compare them with the literature known compounds **SSS** and **PPP**. In addition, spectroelectrochemical IR measurements were performed and revealed an altered tendency of ligands with mixed S/P donor sets to perform a κ^2/κ^3-isomerization as well as CO release, triggered by oxidation of the respective Mo^0-complex. The experimental findings are supported by DFT calculations and show a pronounced tendency of the Mo^0-complexes **11**–**14** to perform κ^2/κ^3-isomerization upon oxidation prior to CO release. Based on the different solvent and oxidation behavior of complexes **11**–**14**, we expected an altered influence when using the ligands in catalytic applications. We subsequently tested the possibility to apply compounds **SSS**, **PPP**, **PSS** and **PPS** as ligands for $Fe_3(CO)_{12}$ in the hydrosilylation of *N*,*N*-dimethylbenzamide to *N*,*N*-dimethylbenzylamine with Ph_2SiH_2. Clearly, the subtle exchange of the substituents has an effect on this reduction. While we solely presented one catalysis example showing different reaction behavior, it is obvious that literature reported catalytic systems based on Triphos (**PPP**) can be further altered in their efficiency and reactivity for numerous processes when altering the donor sets. We expect these findings to further stimulate the application of compounds **SSS**, **PPP**, **PSS** and **PPS** in future catalytic applications.

Experimental

General

All reactions were performed under a dry Ar atmosphere by using standard Schlenk techniques or by working in a Glovebox. Starting materials were obtained from commercial suppliers and used without further purification. Prior to use, all solvents were dried and degassed according to standard methods. $Mo(CO)_3$(toluene), compounds **SSS**,[44,61] **7**[46] and **10**[20] as well as $[Ni(CH_3CN)_6](BF_4)_2$ [62] were synthesized according to literature-known procedures.

(2-Methyl-2-((phenylthio)methyl)propane-1,3-diyl)-bis-(phenylsulfane) SSS

A suspension of 1,1,1-tris(chloro-methyl)ethane (**1**) (3 g, 17.09 mmol) and KI (8.51 g, 51.27 mmol) in 40 mL DMF was cooled to 0 °C. Subsequently, thiophenol (5.23 mL, 5.65 g, 51.27 mmol) was slowly added to a suspension of NaH (60% in mineral oil, 2.05 g, 51.27 mmol) in 20 mL DMF. The thiolate suspension was then added dropwise to the reaction mixture containing **1** and KI. The reaction was heated at 50 °C for 2 d, followed by the addition of 160 mL ethyl acetate. The organic phase was extracted with 2 × 200 mL 1 M NaOH/brine (1 : 1) and dried over anhydrous Na_2SO_4. The solvent was removed in vacuum and the oily residue purified by column chromatography (hexanes/$CHCl_3$, 10 : 3) to yield **SSS** as a colorless oil (3.86 g, 57%). ^{1}H NMR (200 MHz, $CDCl_3$): δ 1.14 (s, 3H, CH_3), 3.13 (s, 6H, CH_2), 7.07–7.32 (m, 15H, Ar). $^{13}C\{^1H\}$ NMR (50 MHz, $CDCl_3$): δ 23.98 (s, CH_3), 41.60 (s, Cq), 43.69 (s, CH_2), 126.22 (s, Ar), 128.99 (s, Ar), 129.79 (s, Ar), 137.09 (s, Ar). IR (cm^{-1}): 3074, 2961, 2912, 1584, 1481, 1438, 1405, 1156, 1089, 854, 748, 702.

(2-Methyl-3-(phenylthio)-2-((phenylthio)methyl)propyl)-diphenyl-phosphane PSS

KO^{t}Bu (0.38 g, 3.42 mmol) was suspended in 20 mL DMSO followed by the addition of $HPPh_2$ (0.60 mL, 3.42 mmol) to afford a red colored solution. The mixture was stirred for 20 min at room temperature and added to a solution of (2-(chloromethyl)-2-methylpropane-1,3-diyl)bis(phenylsulfane) (**4**) (1.00 g, 3.11 mmol). The reaction was stirred for 1 d at 100 °C while the solution turned colorless. Subsequently, the solvent was removed and the residue purified by column chromatography (hexane/Et_2O, 9 : 1) to yield compound **PSS** (1.43 g, 97%) as a colorless oil. ^{1}H NMR (200 MHz, $CDCl_3$): δ 1.09 (s, 3H, CH_3), 2.44 (s, 2H, CH_2PPh_2), 3.18 (s, 4H, CH_2SPh), 7.10–7.47 (m, 20H, Ar). $^{31}P\{^1H\}$ NMR (101 MHz, $CDCl_3$): δ −25.58 (s, –PPh_2). $^{13}C\{^1H\}$ NMR (50 MHz, $CDCl_3$): δ 25.69 (d, J = 9.3 Hz), 39.42 (d, J = 15.6 Hz), 40.68 (d, J = 14.4 Hz), 45.42 (d, J = 9.7 Hz), 110.67–139.04 (m, Ar). IR (cm^{-1}): 3054, 3013, 2960, 2913, 1953, 1877, 1806, 1580, 1477, 1431, 736, 690.

(2-Methyl-2-((phenylthio)methyl)propane-1,3-diyl)-bis(diphenylphosphane) PPS

$HPPh_2$ (3.10 mL, 3.31 g, 17.78 mmol) was added dropwise to a suspension of KO^{t}Bu (2.00 g, 17.78 mmol) in 20 mL DMSO to

produce an intense red colored solution. The mixture was stirred at room temperature for 20 min and added to (3-chloro-2-(chloromethyl)-2-methylpropyl)-(phenyl)sulfane (**5**) (2.10 g, 8.47 mmol) in 30 mL DMSO. The reaction was heated at 100 °C for 1 d and subsequently the solvent was removed in vacuum. The oily crude product was purified by column chromatography (hexane/diethyl ether, 9 : 1) to yield **PPS** as a colorless oily product (3.75 g, 80%). ^{1}H NMR (200 MHz, $CDCl_3$): δ 1.04 (s, 3H, CH_3), 2.47 (s, 4H, CH_2PPh_2), 3.18 (s, 2H, CH_2SPh), 7.22–7.51 (m, 25H, Ar). $^{13}C\{^{1}H\}$ NMR (50 MHz, $CDCl_3$): δ 27.73 (t, J = 8.3 Hz, $C_{q.}$), 39.54 (t, J = 13.8 Hz), 41.29 (q, J = 8.8 Hz), 47.00 (t, J = 10.6 Hz), 125.59–139.85 (m, Ar). $^{31}P\{^{1}H\}$ NMR (101 MHz, $CDCl_3$): δ −25.54 (s, PPh_2).

(3-Chloro-2-(chloromethyl)-2-methylpropyl)-diphenylphosphane 2

$HPPh_2$ (1.00 mL, 1.06 g, 5.70 mmol) was added dropwise to a suspension of KO^{t}Bu (0.64 g, 5.70 mmol) in 20 mL DMSO to produce an intense red colored solution. The mixture was stirred at room temperature for 30 min and added to 1,3-dichloro-2-(chloromethyl)-2-methylpropane (**1**) (1.00 g, 5.70 mmol) in 60 mL DMSO. The reaction was heated at 100 °C for 1 d and subsequently the solvent was removed in vacuum. The oily crude product was purified by column chromatography (hexane/toluene, 2 : 1) to yield **2** as colorless oily product (1.33 g, 72%). ^{1}H NMR (200 MHz, $CDCl_3$): δ 1.03 (s, 3H; CH_3), 2.27 (d, J = 3.98 Hz, 2H, CH_2PPh_2), 3.58 (q, J = 11.03 Hz, 4H, CH_2Cl), 7.12–7.50 (m, Ar). $^{13}C\{^{1}H\}$ NMR (50 MHz, CDCl3): δ 22.15 (d, J = 9.92 Hz, CH_3), 35.87 (d, J = 17.61 Hz, $C_{q.}$), 40.68 (d, J = 14.28 Hz, CH_2PPh_2), 51.47 (d, 10.76 Hz, CH_2Cl), 128.63–138.33 (m, Ar). $^{31}P\{^{1}H\}$ NMR (100 MHz, $CDCl_3$): δ −26.24 (s, PPh_2).

(2-(Chloromethyl)-2-methylpropane-1,3-diyl) bis(diphenyl-phosphane) 3

KO^{t}Bu (1.28 g, 11.40 mmol) was suspended in 20 mL DMSO followed by the addition of $HPPh_2$ (2.00 mL, 2.12 g, 11.40 mmol) to afford a red colored solution. After stirring at room temperature for 15 min the solution was added slowly to a mixture of 1,3-dichloro-2-(chloromethyl)-2-methylpropane (**1**) (1.00 g, 5.70 mmol) in 60 mL DMSO. The mixture was stirred at 100 °C for 1 d and the solvent was removed in vacuum. The obtained oily residue was purified by column chromatography (hexane/toluene, 1 : 1) to yield colorless oily **3** (0.65 g, 24%). ^{1}H NMR (200 MHz, $CDCl_3$): δ 0.98 (s, 3H; CH_3), 2.35 (s, 4H, CH_2PPh_2), 3.68 (s, 2H, CH_2Cl), 7.15–7.46 (m, Ar). $^{13}C\{^{1}H\}$ NMR (50 MHz, $CDCl_3$): δ 21.82 (s, CH_3), 26.05 (t, J = 9.31 Hz, $C_{q.}$), 39.99 (m, J = 8.91 Hz, CH_2PPh_2), 55.29 (m, 11.65 Hz, CH_2Cl), 125.68–139.34 (m, Ar). $^{31}P\{^{1}H\}$ NMR (100 MHz, $CDCl_3$): δ −25.60 (s, PPh_2).

(2-(Chloromethyl)-2-methylpropane-1,3-diyl)bis-(phenyl-sulfane) 4

A suspension of compound **1** (3 g, 17.24 mmol) and KI (5.73 g, 34.50 mmol) in 40 mL DMF was cooled to 0 °C. Subsequently, thiophenol (3.60 mL, 3.80 g, 34.50 mmol) was slowly added to NaH (60% in mineral oil, 1.38 g, 34.50 mmol) suspended in 15 mL DMF. The obtained thiolate suspension was then added dropwise to the mixture containing KI and **1**. The reaction mixture was kept at 50 °C for 2 d. Subsequently, 160 mL ethyl acetate were added to the reaction mixture, the organic phase was extracted with 2 × 200 mL 1 M NaOH/brine (1 : 1) and dried over anhydrous Na_2SO_4. The solvent was removed in vacuum and the residue purified by column chromatography (hexane/$CHCl_3$, 10 : 3) to yield compound **4** as colorless oily product (2.30 g, 42%). ^{1}H NMR (250 MHz, $CDCl_3$): δ 1.07 (s, 3H, CH_3), 3.04 (s, 4H, CH_2), 3.55 (s, 2H, CH_2Cl), 7.05–7.31 (m, 10H, Ar). $^{13}C\{^{1}H\}$ NMR (63 MHz, $CDCl_3$): δ 22.32 (s, CH_3), 41.90 (s, $C_{q.}$), 42.33 (s, CH_2SPh), 51.47 (s, CH_2Cl), 126.51 (s, Ar), 129.10 (s, Ar), 130.10 (s, Ar), 136.77 (s, Ar). IR (cm^{-1}): 3058, 2965, 1583, 1480, 1438, 1376, 1301, 1089, 1067, 1025, 735, 689.

(3-Chloro-2-(chloromethyl)-2-methylpropyl)(phenyl)sulfane 5

Compound **5** was synthesized according to the procedure described for compound **4**. When compound **1** (2.5 g, 14.25 mmol), KI (2.37 g, 14.25 mmol), thiophenol (1.45 mL, 1.57 g, 14.24 mmol) and NaH (60% in mineral oil, 0.57 g, 14.24 mmol) reacted under otherwise identical conditions, compound **4** was obtained as a colorless oil (1.94 g, 55%) ^{1}H NMR (200 MHz, $CDCl_3$): δ 1.15 (s, 3H, CH_3), 3.08 (s, 2H, CH_2SPh), 3.59 (d, 4H, J = 2.5 Hz, CH_2Cl), 7.14–7.43 (m, 5H). $^{13}C\{^{1}H\}$ NMR (50 MHz, $CDCl_3$): δ 20.76 (s, CH_3), 41.01 (s, $C_{q.}$), 42.06 (s, CH_2S), 49.88 (s, CH_2Cl), 126.80 (s, Ar), 129.20 (s, Ar), 130.38 (s, Ar), 136.44 (s, Ar). IR (cm^{-1}): 3075, 3059, 2970, 2951, 1583, 1480, 1459, 1438, 1409, 1300, 1089, 1025, 772, 702.

[Ni(PPP)(CH$_3$CN)$_3$](BF$_4$)$_2$ 7

Compound **7** was synthesized following a modified literature reported procedure.[46] Compound **PPP** (100 mg, 0.16 mmol) was dissolved in 4 mL CH_3CN followed by the addition of $[Ni(CH_3CN)_6](BF_4)_2$ (70 mg, 0.16 mmol) dissolved in 2 mL CH_3CN and stirred for 24 h at room temperature. The resulting dark red solution was evaporated to dryness and the residue then dissolved in CH_3CN. Crystals of **7** were obtained by slow diffusion of diethyl ether into the CH_3CN solution of **7**. The dark red crystals obtained were filtered off, washed with hexane and diethyl ether and dried in a vacuum to yield 137 mg (86%) of compound **7**. ESI-MS. Calcd for $[C_{41}H_{39}NiP_3 + H_2O]^+$: 701.4. Found: 701.1. IR (KBr, cm^{-1}): 3053, 1483, 1435, 1284, 1121, 1060, 993, 797, 744, 695. UV/vis: 422 nm (ε = 1490 L mol^{-1} cm^{-1}), 728 nm (ε = 460 L mol^{-1} cm^{-1}).

[Ni(PPS)(CH$_3$CN)$_2$](BF$_4$)$_2$ 8

Compound **PPS** (23 mg, 0.042 mmol) was dissolved in CH_3CN followed by the addition of $Ni(CH_3CN)_6(BF_4)_2$ (20 mg, 0.042 mmol). The resulting dark red solution was stirred at room temperature overnight. Subsequently, the reaction mixture was filtered and the solvent removed. The solid was recrystallized from CH_3CN and diethyl ether to afford complex **6** as red crystalline solid (20 mg, 55%). ^{1}H NMR (200 MHz, $CDCl_3$): δ 1.13 (s, 3H, CH_3), 2.49 (s, 4H, CH_2PPh_2), 2.82 (s, 4H, CH_2SPh), 7.48 (m, Ar). $^{13}C\{^{1}H\}$ NMR (50 MHz, $CDCl_3$): δ 15.19

(s, $C_{q.}$), 25.18 (s, CH_3), 38.42 (s, CH_2PPh_2), 47.88 (s, CH_2SPh), 57.35 (s, CH_3), 180.35–189.82 (m, Ar). $^{31}P\{^1H\}$ NMR (100 MHz, $CDCl_3$): δ 15.20 (s, PPh_2). IR(cm^{-1}): 3067, 2989, 2930, 2339, 1427, 1048, 734, 699. UV/vis: 428 nm (ε = 532 L mol^{-1} cm^{-1}). Calcd for $[C_{39}H_{40}N_2NiP_2S]$: C 67.94%; H 5.85%; N 4.06%; S 4.65%. Found: C 67.2%; H 5.1%; N 4.5%; S 3.9%.

[Fe(PPS)Cl_2] 9

Compound **PPS** (50 mg, 0.0912 mmol) was suspended in 2 mL THF and $FeCl_2$ (12 mg, 0.0912 mmol) was added in one portion. The formed dark red solution was then stirred at room temperature overnight. The reaction mixture was filtered and the solvent removed in vacuum. The resulting dark red solid was recrystallized from THF by diethyl ether diffusion. The crystals were separated and dried to afford 34 mg (55%) of complex **9**. $^{13}C\{^1H\}$ NMR (50 MHz, $CDCl_3$): δ −18.36 (s, CH_3), −14.57, −12.68, 6.25, 100.89–104.65 (Ar). IR(cm^{-1}): 3053, 2922, 1580, 1478, 1432, 1237, 1184, 1093, 1024, 991, 822, 738, 691. Calcd for $[C_{35}H_{34}FeP_2SCl_2]$: C 62.24%; H 5.07%; S 4.75. Found: C 62.1%; H 5.0%; S 4.2%.

[Mo(SSS)$(CO)_3$] 11

Compound **SSS** (150 mg, 0.38 mmol) was dissolved in 4 mL THF followed by the addition of Mo$(CO)_3$(toluene) (102 mg, 0.38 mmol) in 2 mL dry THF. The obtained light yellow solution was stirred at room temperature. After 24 h, the solvent was reduced to ~1/5 of its original volume and maintained at 0 °C to obtain yellow crystals. The obtained crystals were then washed with diethyl ether and dried in vacuum to afford compound **11** as bright yellow crystalline compound (173 mg, 79%). ^1H NMR ($CDCl_3$, 200 MHz): δ 1.11 (s, 3H, CH_3), 3.10 (s, 6H, CH_2SPh), 7.12–7.54 (m, Ar). $^{13}C\{^1H\}$ NMR (50 MHz, $CDCl_3$): δ 8.41 (s, $C_{q.}$), 25.63 (s, CH_3), 43.65 (s, CH_2SPh), 126.14–137.00 (m, Ar). IR (cm^{-1}): 3060, 2966, 2924, 2865, 1925, 1821, 1791, 1439, 1065, 1013, 740, 687. Calcd for $[C_{26}H_{24}MoO_3S_3]$: C 54.16%; H 4.20%; S 16.68%. Found: C 53.7%; H 4.1%; S 16.2%.

[Mo(PSS)$(CO)_3$] 12

Compound **PSS** (50 mg, 0.106 mmol) was dissolved in 6 mL THF followed by the addition of Mo$(CO)_3$(toluene) (28 mg, 0.106 mmol) in 6 mL THF. The mixture turned dark yellow and was stirred overnight. The reaction mixture was filtered and the solvent removed in vacuum. The yellow solid was recrystallized from THF by diethyl ether diffusion. The obtained crystals were washed with diethyl ether and dried in vacuum to afford complex **12** as crystalline solid (20 mg, 28%). $^{31}P\{^1H\}$ NMR (100 MHz, $CDCl_3$): δ 18.50 (s, PPh_2). IR (cm^{-1}): 3054, 2960, 2924, 2859, 1926, 1837, 1788, 1432, 1090, 729, 693. Calcd for $[C_{32}H_{29}MoO_3PS_2]$: C 58.89%; H 4.48%; S 9.82%. Found: C 58.6%; H 4.22%, S 9.54%.

[Mo(PPS)$(CO)_3$] 13

Compound **PPS** (1.00 g, 1.82 mmol) was dissolved in 10 mL THF followed by the addition of Mo$(CO)_3$(toluene) (496 mg, 1.82 mmol) in 5 mL dry THF. The formed light yellow solution was stirred for 24 h at room temperature. Subsequently, the solvent was removed and the obtained residue dissolved in THF. Addition of hexane led to precipitation of crude **13**, which was then recrystallized by diffusion of THF into a hexane solution (1.26 g, 95%). ^1H NMR (200 MHz, $CDCl_3$): δ 1.13 (s, 3H, CH_3), 2.36 (s, 4H, CH_2PPh_2), 2.75 (s, 2H, CH_2SPh), 7.19–7.53 (m, Ar). $^{13}C\{^1H\}$ NMR (50 MHz, $CDCl_3$): δ 12.68 (s, $C_{q.}$), 7.00 (s, CH_3), 49.33 (s, CH_2SPh), 53.49 (s, CH_2PPh_2), 172.88–191.23 (m, Ar). $^{31}P\{^1H\}$ NMR (100 MHz, $CDCl_3$): δ 18.08 (s, PPh_2). IR (cm^{-1}): 3054, 2972, 2924, 2859, 1925, 1829, 1818, 1474, 1432, 1090, 746, 693. Calcd for $[C_{38}H_{34}MoO_3P_2S]$: C 62.64%; H 4.70%; S 4.40%. Found: C 62.6%; H 5.0%; S 4.1%.

[Mo(PPP)$(CO)_3$] 14

Compound **PPP** (1.00 g, 1.60 mmol) was dissolved in 10 mL THF followed by the addition of Mo$(CO)_3$(toluene) (435 mg, 1.60 mmol) dissolved in 5 mL THF. The obtained yellow solution was stirred at room temperature for additional 24 h. The solvent was removed in vacuum and the obtained residue dissolved in THF. Crude complex **14** was precipitated by addition of hexane. The product was then recrystallized by diffusion of THF into a hexane solution of **14** and afforded 515 mg (40%) of the desired product as yellow crystalline solid. ^1H NMR (200 MHz, $CDCl_3$): δ 1.44 (s, 3H; CH_3), 2.41 (s, 6H, CH_2PPh), 7.07–7.35 (m, 30H, Ar). $^{31}P\{^1H\}$ NMR (100 MHz, $CDCl_3$): δ 18.32 (s, PPh_2). IR (cm^{-1}): 3078, 3042, 2948, 2894, 2859, 1925, 1831, 1803, 1480, 1432, 1084, 740, 687. Calcd for $[C_{26}H_{24}MoO_3S_3]$: C 65.68%; H 4.89%. Found: C 65.6%; H 4.4%.

Catalytic reduction of *N*,*N*-dimethylbenzamide to *N*,*N*-dimethylbenzylamine

$Fe_3(CO)_{12}$ (2 mol%) and the respective ligand (2 mol%) were dissolved in 8 mL of toluene. After 5 min of stirring at room temperature, *N*,*N*-dimethylbenzamide (100 mg, 0.67 mmol) and 2 equiv. diphenylsilane were added. The reaction mixture was stirred for 16 h at 100 °C. The conversion to *N*,*N*-dimethylbenzylamine was detected *via* GC-MS and yields determined by external calibration with *N*,*N*-dimethylbenzylamine.

Acknowledgements

This work was supported by the Fonds der Chemischen Industrie (Liebig grant to U.-P. A.) and through the Deutsche Forschungsgemeinschaft (Emmy Noether grant to U.-P. A., AP242/2-1) as well as through the Alexander von Humboldt Foundation (Humboldt Research Fellowship to R. Miller). We thank M. Heller and Dr B. Mallick for valuable support.

Notes and references

1 A. Phanopoulos, P. W. Miller and N. J. Long, *Coord. Chem. Rev.*, 2015, **299**, 39–60.

2 A. Petuker, M. L. Reback and U.-P. Apfel, *Eur. J. Inorg. Chem.*, 2017, DOI: 10.1002/ejic.201700388.
3 B. J. Sarmah and D. K. Dutta, *J. Organomet. Chem.*, 2010, **695**, 781–785.
4 F. M. A. Geilen, B. Engendahl, M. Hölscher, J. Klankermayer and W. Leitner, *J. Am. Chem. Soc.*, 2011, **133**, 14349–14358.
5 S. Imm, S. Bähn, M. Zhang, L. Neubert, H. Neumann, F. Klasovsky, J. Pfeffer, T. Haas and M. Beller, *Angew. Chem., Int. Ed.*, 2011, **50**, 7599–7603.
6 K. Beydoun, G. Ghattas, K. Thenert, J. Klankermayer and W. Leitner, *Angew. Chem., Int. Ed.*, 2014, **53**, 11010–11014.
7 T. vom Stein, M. Meuresch, D. Limper, M. Schmitz, M. Hölscher, J. Coetzee, D. J. Cole-Hamilton, J. Klankermayer and W. Leitner, *J. Am. Chem. Soc.*, 2014, **136**, 13217–13225.
8 S. Wesselbaum, V. Moha, M. Meuresch, S. Brosinski, K. M. Thenert, J. Kothe, T. vom Stein, U. Englert, M. Holscher, J. Klankermayer and W. Leitner, *Chem. Sci.*, 2015, **6**, 693–704.
9 E. J. Derrah, M. Hanauer, P. N. Plessow, M. Schelwies, M. K. da Silva and T. Schaub, *Organometallics*, 2015, **34**, 1872–1881.
10 M. Meuresch, S. Westhues, W. Leitner and J. Klankermayer, *Angew. Chem., Int. Ed.*, 2016, **55**, 1392–1395.
11 B. Erb, E. Risto, T. Wendling and L. J. Gooßen, *ChemSusChem*, 2016, **9**, 1442–1448.
12 I. Mellone, M. Peruzzini, L. Rosi, D. Mellmann, H. Junge, M. Beller and L. Gonsalvi, *Dalton Trans.*, 2013, **42**, 2495–2501.
13 C. Bianchini, A. Meli, M. Peruzzini, F. Vizza, Y. Fujiwara, T. Jintoku and H. Taniguchi, *J. Chem. Soc., Chem. Commun.*, 1988, 299–301.
14 M. Rosales, G. Chacon, A. Gonzalez, I. Pacheco, P. J. Baricelli and L. G. Melean, *J. Mol. Catal.*, 2008, **287**, 110–114.
15 M. Rosales, R. Vallejo, J. Jose Soto, L. Jhonatan Bastidas, K. Molina and P. J. Baricelli, *Catal. Lett.*, 2010, **134**, 56–62.
16 A. B. Chaplin and P. J. Dyson, *Eur. J. Inorg. Chem.*, 2007, 4973–4979.
17 A. B. Chaplin and P. J. Dyson, *Inorg. Chem.*, 2008, **47**, 381–390.
18 H. Broda, J. Krahmer and F. Tuczek, *Eur. J. Inorg. Chem.*, 2014, 3564–3571.
19 H. Broda, S. Hinrichsen, J. Krahmer, C. Nather and F. Tuczek, *Dalton Trans.*, 2014, **43**, 2007–2012.
20 T. J. Korstanje, J. Ivar van der Vlugt, C. J. Elsevier and B. de Bruin, *Science*, 2015, **350**, 298–302.
21 J. Schneidewind, R. Adam, W. Baumann, R. Jackstell and M. Beller, *Angew. Chem., Int. Ed.*, 2017, **56**, 1890–1893.
22 L. Söncksen, C. Gradert, J. Krahmer, C. Näther and F. Tuczek, *Inorg. Chem.*, 2013, **52**, 6576–6589.
23 K. Heinze, G. Huttner, L. Zsolnai and P. Schober, *Inorg. Chem.*, 1997, **36**, 5457–5469.
24 A. Petuker, K. Merz, C. Merten and U.-P. Apfel, *Inorg. Chem.*, 2016, 1183–1191.
25 J. Krahmer, H. Broda, C. Naether, G. Peters, W. Thimm and F. Tuczek, *Eur. J. Inorg. Chem.*, 2011, 4377–4386.
26 S.-T. Liu, H.-E. Wang, M.-C. Cheng and S.-M. Peng, *J. Organomet. Chem.*, 1989, **376**, 333–342.
27 S. T. Liu and K. J. Liu, *Inorg. Chem.*, 1990, **29**, 4576–4579.
28 H. Heidel, G. Huttner and G. Helchem, *Z. Naturforsch., B: J. Chem. Sci.*, 1993, **48**, 1681–1692.
29 W. Hsin-Ell, C. Ming-Chu, L. Gene-Hsiang, P. Shie-Ming and L. Shiuh-Tzung, *J. Organomet. Chem.*, 1993, **445**, 171–179.
30 H. Heidel, J. Scherer, A. Asam, G. Huttner, O. Walter and L. Zsolnai, *Chem. Ber.*, 1995, **128**, 293–301.
31 H. Heidel, G. Huttner and L. Zsolnai, *Z. Naturforsch., B: J. Chem. Sci.*, 1995, **50**, 729–734.
32 O. P. Siclovan and R. J. Angelici, *Inorg. Chem.*, 1998, 432–444.
33 R. Soltek, G. Huttner, L. Zsolnai and A. Driess, *Inorg. Chim. Acta*, 1998, **269**, 143–156.
34 H. W. Yim, L. M. Tran, E. E. Pullen, D. Rabinovich, L. M. Liable-Sands, T. E. Concolino and A. L. Rheingold, *Inorg. Chem.*, 1999, **38**, 6234–6239.
35 S. Batke, T. Kothe, M. Haas, H. Wadepohl and J. Ballmann, *Dalton Trans.*, 2016, **45**, 3528–3540.
36 A. Muth, O. Walter, G. Huttner, A. Asam, L. Zsolnai and C. Emmerich, *J. Organomet. Chem.*, 1994, **468**, 149–163.
37 V. Körner, G. Huttner, L. Zsolnai, M. Büchner, A. Jacobi and D. Günauer, *Chem. Ber.*, 1996, **129**, 1587–1601.
38 S. Beyreuther, A. Frick, J. Hunger, G. Huttner, B. Antelmann, P. Schober and R. Soltek, *Eur. J. Inorg. Chem.*, 2000, 597–615.
39 M. A. Fox, K. A. Campbell and E. P. Kyba, *Inorg. Chem.*, 1981, **20**, 4163–4165.
40 T. Maina, A. Pecorale, A. Dolmella, G. Bandoli and U. Mazzi, *J. Chem. Soc., Dalton Trans.*, 1994, 2437–2443.
41 N. Salvarese, N. Morellato, A. Venzo, F. Refosco, A. Dolmella and C. Bolzati, *Inorg. Chem.*, 2013, **52**, 6365–6377.
42 C. Strohmann, S. Lüdtke and O. Ulbrich, *Organometallics*, 2000, **19**, 4223–4227.
43 P. K. Dornan, P. L. Leung and V. M. Dong, *Tetrahedron*, 2011, **67**, 4378–4384.
44 S. Herold, A. Mezzetti, L. M. Venanzi, A. Albinati, F. Lianza, T. Gerfin and V. Gramlich, *Inorg. Chim. Acta*, 1995, **235**, 215–231.
45 E. N. Tsvetkov, N. A. Bondarenko, I. G. Malakhova and M. I. Kabachnik, *Synthesis*, 1986, 198–208.
46 A. Petuker, S. Mebs, N. Schuth, P. Gerschel, M. L. Reback, B. Mallick, M. van Gastel, M. Haumann and U.-P. Apfel, *Dalton Trans.*, 2017, **46**, 907–917.
47 E. J. Hawrelak, W. H. Bernskoetter, E. Lobkovsky, G. T. Yee, E. Bill and P. J. Chirik, *Inorg. Chem.*, 2005, **44**, 3103–3111.
48 R. Langer, F. Bönisch, L. Maser, C. Pietzonka, L. Vondung and T. P. Zimmermann, *Eur. J. Inorg. Chem.*, 2015, **2015**, 141–148.

49 A. Barton, J. Connolly, W. Levason, A. Mendia-Jalon, S. Orchard and G. Reid, *Polyhedron*, 2000, **19**, 1373–1379.
50 D. Sellmann and J. Schwarz, *J. Organomet. Chem.*, 1983, **241**, 343–361.
51 S. Dilsky, *J. Organomet. Chem.*, 2007, **692**, 2887–2896.
52 A. C. Kautz, P. C. Kunz and C. Janiak, *Dalton Trans.*, 2016, **45**, 18045–18063.
53 N. A. F. Al-Rawashdeh, S. Chatterjee, J. A. Krause and W. B. Connick, *Inorg. Chem.*, 2014, **53**, 294–307.
54 S. V. Timofeev, O. B. Zhidkova, E. M. Mosolova, I. B. Sivaev, I. A. Godovikov, K. Y. Suponitsky, Z. A. Starikova and V. I. Bregadze, *Dalton Trans.*, 2015, **44**, 6449–6456.
55 P. Dyer, J. Fawcett, M. Hanton, R. Kemmitt, R. Padda and N. Singh, *Dalton Trans.*, 2003, 104–113.
56 F. Xu, C. Tard, X. Wang, S. K. Ibrahim, D. L. Hughes, W. Zhong, X. Zeng, Q. Luo, X. Liu and C. J. Pickett, *Chem. Commun.*, 2008, 606–608.
57 M. C. Durrant, B. Goerdt, C. Hauser, T. Krawinkel and R. L. Richards, *Transition Met. Chem.*, 1995, **20**, 583–589.
58 J. D. Seixas, A. Mukhopadhyay, T. Santos-Silva, L. E. Otterbein, D. J. Gallo, S. S. Rodrigues, B. H. Guerreiro, A. M. L. Goncalves, N. Penacho, A. R. Marques, A. C. Coelho, P. M. Reis, M. J. Romao and C. C. Romao, *Dalton Trans.*, 2013, **42**, 5985–5998.
59 S. Zhou, K. Junge, D. Addis, S. Das and M. Beller, *Angew. Chem., Int. Ed.*, 2009, **48**, 9507–9510.
60 B.-H. Zhu, G.-H. Xu and Z.-W. Xia, in *Adv. Chem. Engineering, PTS 1-3*, ed. Y. X. Wen, and F. H. Lei, Guangxi Univ, China; Wuhan Univ Sci & Technol, China; Queensland Univ Technol, Australia, 2012, vol. 396–398, pp. 2485–2488.
61 A. Petuker, C. Merten and U.-P. Apfel, *Eur. J. Inorg. Chem.*, 2015, 2139–2144.
62 B. J. Hathaway, D. G. Holah and A. E. Underhill, *J. Chem. Soc.*, 1962, 2444–2448.